Research Article | Vol. 24, No. 15 | 25 Jul 2016 | OPTICS EXPRESS 17760

Optics EXPRESS

Broadband gold nanoantennas arrays with transverse dimension effects

CHEN-WEI SU[1] AND KUO-PING CHEN[2,*]

[1]Institute of Photonic System, National Chiao Tung University, Taiwan
[2]Institute of Imaging and Biomedical Photonics, National Chiao Tung University, Taiwan
[*]kpchen@nctu.edu.tw

Abstract: Broadband resonance in gold paired-rods nanoantennas and paired-strips gratings is investigated when the nanostructure's transverse (non-polarization) dimension is changed from paired-rods to paired-strips. Increasing the transverse dimension blue shifts the resonance wavelength and widens its bandwidth due to cancellation of the magnetic field between nanoantennas. A derived resistor-inductor-capacitor (RLC) equivalent circuit model verifies the nanostructures' resonance when elongating the transverse dimensions. Paired-strips gratings have a bandwidth 2.04 times that of paired-rods nanoantennas.

OCIS codes: (250.5403) Plasmonics; (160.3918) Metamaterials; (250.0250) Optoelectronics.

References and links

1. H. Duan, A. I. Fernández-Domínguez, M. Bosman, S. A. Maier, and J. K. Yang, "Nanoplasmonics: classical down to the nanometer scale," Nano Lett. **12**(3), 1683–1689 (2012).
2. Z.-Y. Yang and K.-P. Chen, "Effective absorption enhancement in dielectric thin-films with embedded paired-strips gold nanoantennas," Opt. Express **22**(11), 12737–12749 (2014).
3. R. M. Bakker, A. Boltasseva, Z. Liu, R. H. Pedersen, S. Gresillon, A. V. Kildishev, V. P. Drachev, and V. M. Shalaev, "Near-field excitation of nanoantenna resonance," Opt. Express **15**(21), 13682–13688 (2007).
4. Y.-H. Chen, K.-P. Chen, M.-H. Shih, and C.-Y. Chang, "Observation of the high-sensitivity plasmonic dipolar antibonding mode of gold nanoantennas in evanescent waves," Appl. Phys. Lett. **105**(3), 031117 (2014).
5. W. Li, U. Guler, N. Kinsey, G. V. Naik, A. Boltasseva, J. Guan, V. M. Shalaev, and A. V. Kildishev, "Refractory plasmonics with titanium nitride: broadband metamaterial absorber," Adv. Mater. **26**(47), 7959–7965 (2014).
6. E. S. Unlü, R. U. Tok, and K. Şendur, "Broadband plasmonic nanoantenna with an adjustable spectral response," Opt. Express **19**(2), 1000–1006 (2011).
7. R. S. Penciu, K. Aydin, M. Kafesaki, T. Koschny, E. Ozbay, E. N. Economou, and C. M. Soukoulis, "Multi-gap individual and coupled split-ring resonator structures," Opt. Express **16**(22), 18131–18144 (2008).
8. M. Navarro-Cia and S. A. Maier, "Broad-band near-infrared plasmonic nanoantennas for higher harmonic generation," ACS Nano **6**(4), 3537–3544 (2012).
9. K. Aydin, V. E. Ferry, R. M. Briggs, and H. A. Atwater, "Broadband polarization-independent resonant light absorption using ultrathin plasmonic super absorbers," Nat. Commun. **2**, 517 (2011).
10. R. U. Tok and K. Şendur, "Plasmonic spiderweb nanoantenna surface for broadband hotspot generation," Opt. Lett. **39**(24), 6977–6980 (2014).
11. Y. Sun, B. Edwards, A. Alù, and N. Engheta, "Experimental realization of optical lumped nanocircuits at infrared wavelengths," Nat. Mater. **11**(3), 208–212 (2012).
12. H. Caglayan, S.-H. Hong, B. Edwards, C. R. Kagan, and N. Engheta, "Near-infrared metatronic nanocircuits by design," Phys. Rev. Lett. **111**(7), 073904 (2013).
13. H. Fischer and O. J. Martin, "Engineering the optical response of plasmonic nanoantennas," Opt. Express **16**(12), 9144–9154 (2008).
14. G. W. Bryant, F. J. García de Abajo, and J. Aizpurua, "Mapping the plasmon resonances of metallic nanoantennas," Nano Lett. **8**(2), 631–636 (2008).
15. L. Wang and Z. M. Zhang, "Effect of magnetic polaritons on the radiative properties of double-layer nanoslit arrays," J. Opt. Soc. Am. B **27**(12), 2595–2604 (2010).
16. T. D. Corrigan, P. W. Kolb, A. B. Sushkov, H. D. Drew, D. C. Schmadel, and R. J. Phaneuf, "Optical plasmonic resonances in split-ring resonator structures: an improved LC model," Opt. Express **16**(24), 19850–19864 (2008).
17. I. Wang and Y.-p. Du, "Optical input impedance of nanostrip antennas," Opt. Eng. **51**, 054002 (2012).
18. A. Alù and N. Engheta, "Input impedance, nanocircuit loading, and radiation tuning of optical nanoantennas," Phys. Rev. Lett. **101**(4), 043901 (2008).
19. C. P. Huang, X. G. Yin, H. Huang, and Y. Y. Zhu, "Study of plasmon resonance in a gold nanorod with an LC circuit model," Opt. Express **17**(8), 6407–6413 (2009).
20. L. P. Wang and Z. M. Zhang, "Phonon-mediated magnetic polaritons¶in the infrared region," Opt. Express **19**(S2), A126–A135 (2011).

#265318 http://dx.doi.org/10.1364/OE.24.017760
Journal © 2016 Received 16 May 2016; revised 21 Jul 2016; accepted 24 Jul 2016; published 27 Jul 2016

Optics EXPRESS

1. Introduction

Nanoscale optoelectronics have been extensively studied in the past decade [1]. One of the most interesting topics in nanophotonics is plasmonic nanoantennas. These antennas are made with noble metals, which exhibit different characteristics in visible or near-infrared (NIR) wavelengths. Nanoantennas have demonstrated enhancement of the near-field intensity from dye molecules and fluorescent materials, enhanced absorption, sensing, and an increased Raman signal [2–4]. It is well known that nanoantennas support narrow band resonance. However, in many novel applications, such as perfect absorbers or metasurfaces [5], the broadband resonance of nanoantenna is essential. In literatures, there are couple ways which could obtain broadband resonance of nanoantennas: (i) bringing particles with different resonance [6]; and (ii) designing structures with coupling of multiple modes [7]. However, in those design, the structures of nanoantennas are complicated which could be a challenge in fabrication [8–10]. In this work, a novel approach to design the broadband nanoantennas by simply changing the transverse dimension is proposed.

In literatures, the most common shapes, like elliptical, bowtie, and disk nanoantennas made of different metals (gold, silver, and aluminum) or nanogratings made of different dielectrics were proposed and investigated [11, 12]. Various resonance wavelengths of nanoantennas can be achieved by adjusting geometric parameters, including thickness, width [13], and gap [14] dimensions between plasmonic nanoantennas. In literatures, it has been focused more on shifting resonance wavelengths of nanoantennas and the electric field enhancement around the structures, but less discussing on controlling bandwidth of resonance. In RF antenna design, a dipole antenna can be made more broadband by increasing the radius of the dipole. However, literatures in optical antennas mainly discussed changing the dimension in the polarization direction of the incident light, while few discuss the same in the non-polarization direction.

In this work, the dimension in the transverse direction of plasmonic nanoantennas was modified while longitudinal resonance was applied to the nanoantenna arrays. An RLC equivalent circuit model is introduced to verify the plasmonic coupling effect of paired-rods nanoantennas and paired-strips gratings at resonances in the optical range. In addition, the mutual inductance of nanoantennas arrays is discussed in this manuscript, which has been widely applied in metal-insulator-metal (MIM) [15], split ring resonator (SRR) [16] and gratings structures, but less discussed in nanoantenna arrays.

2. Design and fabrication

Gold paired-rods nanoantennas and paired-strips gratings with a period of 400 nm were fabricated on indium tin oxide (ITO) glass substrates using electron beam lithography (EBL). The 200 nm poly methyl methacrylate (PMMA) electro-resist was spin-coated and patterned using electron beam lithography to define an array with an area of 100 × 100 μm^2 for each structure when the exposure dose was 290-330 $\mu C/cm^2$. After development, electron beam deposition was used to deposit 5 and 50 nm thick Ti and Au layer. The undefined PMMA and excess metal were stripped using acetone. Figure 1(a) shows a schematic of the paired-rods nanoantennas and paired-strips gratings. Structural parameters other than the transverse dimensions, which include the width, thickness, and the gap between structures, were fixed. The optimized structural parameters were a 100 nm width, a 50 nm thickness, and a 50 nm gap between antennas. Transverse dimensions of nanoantennas were varied from paired-rods nanoantennas to paired-strips gratings. The applied electromagnetic wave is TM polarized (i.e., the electric field direction is parallel to the x-axis direction). Figures 1(b)-1(e) show scanning electron microscopy (SEM) images of plasmonic paired-rods nanoantennas with different dimensions in the transverse direction and paired-strips gratings.

Optics EXPRESS

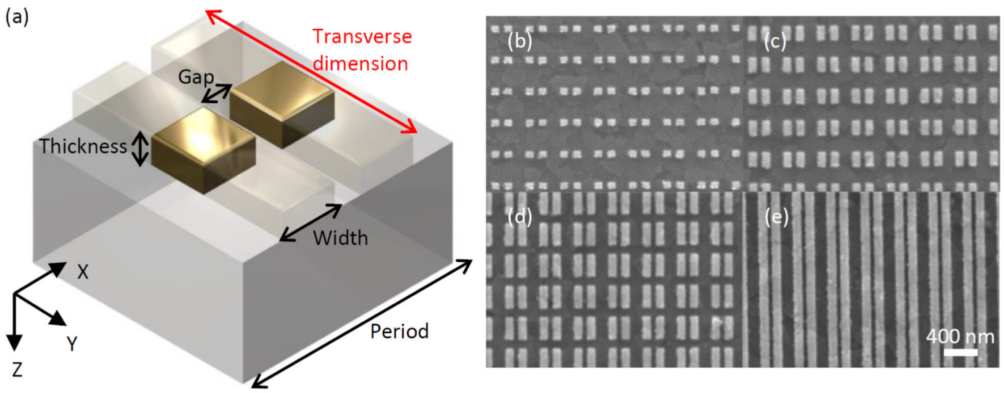

Fig. 1. Schematic of the plasmonic nanoantennas of varying transverse dimensions and SEM images of paired-rods nanoantennas with different transverse dimensions and paired-strips gratings. (a) Schematic diagram of nanoantennas changed from paired-rods to paired-strips. (b) 100 nm, (c) 200 nm, (d) 300 nm, and (e) infinitely long (also called paired-strips gratings).

3. Analysis of transmittance spectra and near field distribution

Paired-rods nanoantenna arrays and paired-strips gratings were measured by a spectrometer (Ocean optics USB 2000 +) for the analysis of transmittance spectra. The measurement results in Fig. 2(a) are compared with simulation results in Fig. 2(b). As indicated in Fig. 2(a), there is a blue shift of the longitudinal resonance when the transverse dimension of the plasmonic nanoantennas is increased. The finite element analysis method (FEM) simulation results in Fig. 2(b) show the same trend as the experimental results. In addition, the bandwidths of nanoantennas are increasing significantly.

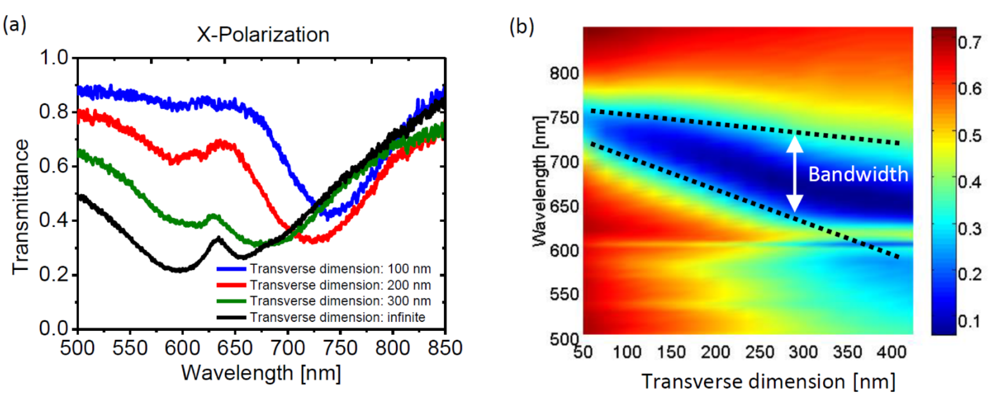

Fig. 2. Transmittance spectra of experiment and simulation results. (a) Transmittance spectra of different transverse dimension nanoantennas in measurement. (b) FEM simulations of two-dimensional (2D) mapping of transmittance spectra with various transverse dimensions.

For the near-field, to analyze the electric field distribution in the plasmonic paired-rods nanoantennas with different transverse dimensions and paired-strips gratings, four incident wavelengths corresponding to the longitudinal resonance frequency for each structure were used. Figure 3 shows the localized electric field enhancements of the nanoantennas, from paired-rods nanoantennas to paired-strips gratings. The maximum value of the electric field distribution decreased when the transverse dimension was increased, which means the shorter transverse dimension nanoantennas have a larger localized electric field when the gaps of nanoantennas are fixed. Notably, the paired-rods nanoantennas have a sharper resonance with higher localized electric field, but the paired-strips gratings have broadband resonance and larger enhancement areas. Table 1 shows the maximum localized electric fields and average electric fields from the host when nanoantennas are with different transverse dimensions.

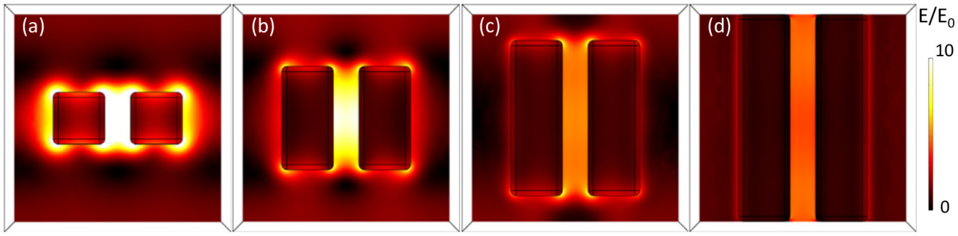

Fig. 3. Enhancements of localized electric fields of paired-rods nanoantennas and paired-strips gratings from the top view. (a) Transverse dimension is 100 nm with wavelength at 720 nm. (b) Transverse dimension is 200 nm with wavelength at 690 nm. (c) Transverse dimension is 300 nm with wavelength at 660 nm. (d) Transverse dimension is 400 nm with wavelength at 645 nm. The value of background electric field (E_0) is approximately about 7×10^7 V/m.

Table 1. Maximum localized electric field and average electric field of gold nanoantennas with different transverse dimensions at the resonance wavelengths.

Nanoantenna Dimensions (x × y)	Maximum Localized Electric Field [V/m]	Average Electric Field [V/m]
100 nm × 100 nm	4.82×10^8	7.71×10^7
100 nm × 200 nm	2.46×10^8	8.0×10^7
100 nm × 300 nm	2.20×10^8	8.2×10^7
paired-strips	1.47×10^8	8.36×10^7

4. Discussions

The impact of varying the transverse dimension of the paired-rods nanoantennas can be explained using RLC equivalent circuit models. Figure 4(a) shows the relationship between the transverse dimension of the nanoantennas and resonance wavelengths of the longitudinal mode. The resonance wavelength moves to shorter wavelengths with increasing transverse dimension in both simulation and experimental results. Figure 4(b) shows the FWHM at resonance frequency, which is calculated by the nonlinear curve fit with Gaussian function from OriginPro. A longer transverse dimension results in a wider resonance frequency FWHM and smaller localized field enhancement. In Fig. 4, the simulation and the experimental results show high correlation with a slightly offset owing to imperfection in sample fabrication.

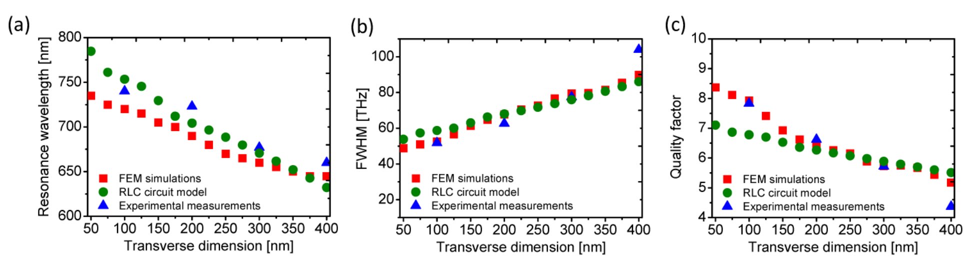

Fig. 4. Simulation (square), experimental (triangle) and RLC circuit model (circle) results for nanoantennas with various transverse dimensions. (a) Resonance wavelengths. (b) FWHM at resonance frequency. (c) Quality factors (Q-factor).

To understand the trend of simulation and experimental results in Fig. 4, equivalent circuit models were derived to analyze the effect of changing the transverse dimension of the nanoantennas. Based on literatures [17, 18], the equivalent circuit model could provide valuable information on the properties of paired-rods nanoantennas and paired-strips gratings. With the equivalent model, which combines metal nanoparticles of negative permittivity and the dielectric gap of positive permittivity, a second-order resonant LC circuit that may oscillate in the NIR and visible frequencies can be obtained. In this study, the RLC equivalent circuit model is used to describe the resonance characteristics of the nanoantennas. The Q-factor can be derived by:

$$Q-factor=\frac{1}{R_0}\sqrt{\frac{L_{eq}}{C_g}} \tag{1}$$

where C_g is the total capacitance, R_0 is the resistance, and L_{eq} is the equivalent inductance. When the inductors of adjacent nanoantennas in y-direction are with parallel displacement current, the mutual inductance due to magnetic fields coupling has to be considered, and the equivalent inductance is given by:

$$L_{eq}=\left(\frac{L_{k1}L_{k2}-L_m{}^2}{L_{k1}+L_{k2}+2L_m}\right) \tag{2}$$

In this study, the incident light is x-polarized. Therefore, the electric displacement current would flow in the metal in x-direction. This displacement current induced a directionally opposite magnetic field in the intermediate area between the adjacent nanorods in y-direction as shown in Fig. 5(a) and the equivalent circuit model has been shown in Fig. 5(b).

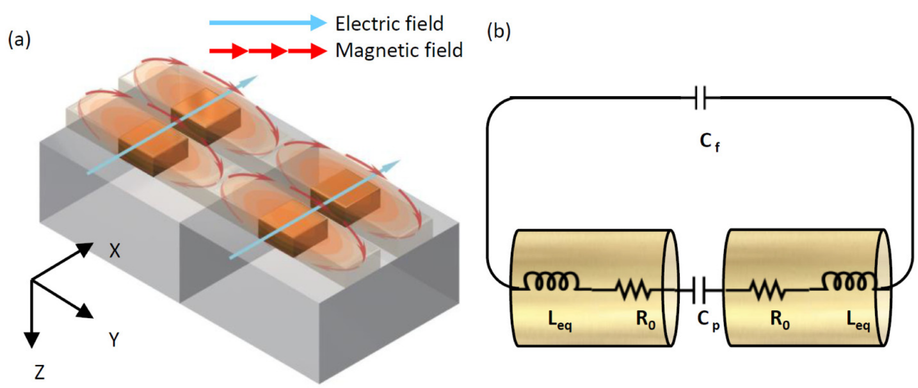

Fig. 5. Optical nanoantenna circuit models. (a) Opposite magnetic fields in the intermediate area between the adjacent nanoantennas in y-direction. (b) Equivalent RLC circuits for the plasmonic paired-rods nanoantennas and paired-strips gratings.

The kinetic inductance (L_k) arises from the inertia of the electrons in a metal, which dominates over the faraday inductance and plays an important role in high frequency fields while interacting with metals. L_{k1} and L_{k2} represent the kinetic inductance for adjacent nanoantennas in y-direction, respectively. L_m is the mutual inductance that exists between the two nanoantennas due to magnetic fields coupling. In addition, the total capacitance (C_g) is combined with the parallel-plate capacitor of the gap and also the fringing fields. Because of their geometric dependency, the total capacitance, resistance and kinetic inductance can be obtained directly as:

$$C_g=C_p+C_f=\varepsilon_{host}\varepsilon_0\frac{tl}{g}+\alpha\pi(\varepsilon_{host}+\varepsilon_{sub})\varepsilon_0 l \tag{3}$$

$$R_0=\frac{w}{\sigma_0 tl} \tag{4}$$

Optics EXPRESS

$$L_k = \frac{\mu_0 w}{\left(\frac{\omega_p}{c}\right)^2 tl} \tag{5}$$

where ε_{host} and ε_{sub} are respectively the relative permittivity of air and ITO glass substrate, ε_0 and μ_0 are permittivity and permeability in free-space, σ_0 and ω_p are conductivity and bulk plasma frequency of gold, c is light velocity, g is the gap between the nanostructures and the *t*, *w* and *l* are the thickness, width and transverse dimension of gold paired-rods nanoantennas and paired-strips gratings. In Eq. (3), the first term (C_p) on the right side is the usual express for the parallel-plate capacitor formed by the gap, and the second tern (C_f) is a correction due to the fringing fields. Based on literatures [19], an appropriate value of $\alpha = 5$ for the gold nanoantennas has been used in this model. Increasing transverse dimensions of nanoantennas would reduce the kinetic inductance [20]. In addition, the amount of flux linkage between adjacent nanostructures can be defined as a fraction of the total possible magnetic flux of each nanoantenna. This fractional value is called the coefficient of coupling (*k*). When increasing the transverse dimension of the nanoantenna, it would strengthen the cancellation of the magnetic field, which increase the mutual inductance. The value of mutual inductance due to the cancellation of the magnetic field from periodic nanoantennas in y-direction is a function of:

$$L_m = k\sqrt{L_{k1}L_{k2}} \tag{6}$$

Generally, *k* is a number between 0 and 1, where 0 means no inductive coupling and 1 indicates full inductive coupling. In this fitting model, the value of *k* is increased from 0.76 to 0.85 when nanostructures are changed from paired-rods nanoantennas to paired-strips gratings. The relationship between the transverse dimension and each circuit component has been listed in Table 2.

Table 2. Geometry dependence of RLC components.

	C_g	R_0	L_k	$k = L_m/L_k$
Increasing transverse dimension	↑	↓	↓	↑

5. Conclusion

In summary, broadband nanoantennas are achieved by elongating the transverse dimensions. The paired-strips gratings exhibited wider bandwidths and also larger enhancement areas. The broadening of resonance is caused by geometry dependence but not material dispersion. Although the Q-factor of paired-strips gratings is less because of the cancellation from mutual inductance, the larger enhancement area of paired-strips gratings could still maintain the effective average field enhancement. The proposed paired-strips gratings are particularly attractive for the broadband applications.

Funding

Ministry of Science and Technology, Taiwan (MOST 104-2221-E-009-130-MY3).

Acknowledgments

The authors would like to thank Dr. Julia Hsin-Lin Lu and Dr. Chin-Lung Yang's helpful discussion about antenna theory, and the support from Prof. Wei Lee for Comsol workstation.